

~~CONFIDENTIAL~~

Copy 287
RM E52F24

~~55-30-62~~

~~NACA~~

DL43315



TECH LIBRARY KAFB, NM

NACA RM E52F24

RESEARCH MEMORANDUM

EXPERIMENTAL INVESTIGATION OF AIR-COOLED TURBINE BLADES
IN TURBOJET ENGINE

XII - COOLING EFFECTIVENESS OF A BLADE WITH AN INSERT
AND WITH FINS MADE OF A CONTINUOUS CORRUGATED SHEET

By Edward R. Bartoo and John L. Clure

Lewis Flight Propulsion Laboratory
Cleveland, Ohio

~~This material contains information affecting the National Defense of the United States within the meaning of the espionage laws, Title 18, U.S.C., and the transmission or revelation of which in any manner to an unauthorized person is prohibited by law.~~

NATIONAL ADVISORY COMMITTEE FOR AERONAUTICS

WASHINGTON
August 28, 1952

~~CONFIDENTIAL~~

310921/2

~~4488 4/24~~

6750

1J
NACA RM E52F24CONFIDENTIAL
NATIONAL ADVISORY COMMITTEE FOR AERONAUTICSRESEARCH MEMORANDUMEXPERIMENTAL INVESTIGATION OF AIR-COOLED TURBINE BLADES
IN TURBOJET ENGINEXII - COOLING EFFECTIVENESS OF A BLADE WITH AN INSERT
AND WITH FINS MADE OF A CONTINUOUS CORRUGATED SHEET

By Edward R. Bartoo and John L. Clure

SUMMARY

An investigation was conducted in a modified turbojet engine to determine the cooling effectiveness of an air-cooled turbine-rotor blade employing a corrugated metal sheet brazed to the inner surface of the blade shell to increase the internal heat-transfer area. An insert blocking the central portion of the cooling passage permitted the use of short corrugations of uniform height, improved coolant distribution, and increased cooling effectiveness.

The corrugated-fin blade had, over a range of coolant-flow ratios, a lower integrated average wall temperature at the section investigated than the more promising shell-supported blade types previously investigated at the NACA Lewis laboratory. Comparison was also made with an air-cooled blade in which the shell was supported by a finned strut within the cooling passage. At rated engine speed, 11,500 rpm, with effective gas and coolant temperatures of 1450° and 180° F, respectively, and a coolant-flow ratio of 0.03, the integrated average wall temperature of the wall (stress-carrying member) of the corrugated-fin blade was 830° F as compared with 930° F for the wall of the shell-supported tube-filled blade and 615° F for the internal strut (stress-carrying member) of the strut-supported blade. At these same conditions comparison was made on the basis of stress ratio factor, which is indicative of load-carrying ability. The corrugated-fin blade was superior to both the shell-supported tube-filled and the strut-supported blades at coolant-flow ratios above 0.01, while both the corrugated-fin and the strut-supported blades appeared capable of safe operation at coolant-flow ratios on the order of 0.01.

CONFIDENTIAL

~~CONFIDENTIAL~~

INTRODUCTION

In a series of investigations being conducted at the NACA Lewis laboratory in modified turbojet engines to determine effective means of air-cooling gas-turbine blades, a number of blade configurations have been investigated in the search for one with high cooling effectiveness, satisfactory durability, reasonable pressure-loss characteristics, and good fabrication possibilities. The midchord cooling effectiveness of a finned blade (reference 1) was found to be superior to that of any of the other shell-supported blades that had been investigated at the NACA; however, the method of fabrication was not simple, and the chordwise temperature gradients were high. The majority of other shell-supported blades that have been investigated (references 2 to 9) utilized tubes brazed to the inner surfaces of the blade shell to augment the internal heat-transfer surface. It was found that the use of thin formed blade shells permitted substantial reductions in the lengths of uncooled leading and trailing edges over those which could be obtained by the casting processes previously employed; the resulting leading- and trailing-edge temperatures were lower and the chordwise temperature gradients were reduced (reference 9). A few of the better designs of tube-filled blades have achieved substantial reductions in blade wall temperatures and have demonstrated satisfactory durability (references 8 and 9); however, further gains in cooling effectiveness were believed possible through improved bonding between shell and tubes and through more nearly optimum arrangement of internal finning.

The strut-supported blade of reference 10 showed extremely good cooling characteristics and offers more promise from the standpoint of heat-transfer than any other air-cooled turbine-rotor blade that has been investigated at the NACA. Further development is required on fabrication methods and blade configurations to improve shell attachment, strut fabrication, and cooling-air-passage arrangements. In general, strut-supported turbine blades are expected to be heavier than the shell-supported type because of the necessity of incorporating an internal supporting member to carry the weight of the shell. For some applications shell-supported blades will be more desirable; consequently, additional research is being carried forward on improved types of shell-supported blades.

In order to combine the cooling effectiveness of the finned blade shown in reference 1 with the reduction of chordwise temperature gradients obtained by the use of thin formed shells as discussed in reference 9 and at the same time to simplify the fabrication method previously used on the finned blade, a new finned-blade configuration was designed, fabricated, and tested in a turbojet engine to determine its temperature distribution and estimated stress-carrying characteristics. This blade utilized a formed shell to which was brazed a thin uniformly corrugated sheet of mild steel to provide additional cooling

surface. The central portion of the interior was blocked off to permit the use of uniform corrugations in the sheet making up the fins and to restrict the coolant flow to the region immediately adjacent to the shell, which limitation was expected to result in a more efficient use of the cooling air. This blade will be referred to in this report as the corrugated-fin blade with an insert or, more simply, the corrugated-fin blade.

This report presents comparisons of the experimentally measured peripheral-temperature distributions, cooling effectiveness, estimated load-carrying ability, and coolant pressure losses of the corrugated-fin blade with those of previously investigated blades.

The data obtained in this investigation of the corrugated-fin blade in a turbojet engine were for a range of engine speeds from 4000 to 11,500 rpm and a maximum range of cooling-air-to-combustion-gas flow ratios from 0.014 to 0.04 at approximately sea-level ambient conditions. The pressure-drop investigation was conducted in a nonrotating modified turbine wheel and engine tail cone for a range of air-flow rates from 0.015 to 0.090 pound per second. These air-flow rates were equivalent to cooling-air-to-combustion-gas flow ratios of 0.011 and 0.068 at the rated engine speed of 11,500 rpm with standard sea-level inlet conditions.

SYMBOLS

The following symbols are used in this report:

- p' total pressure, lb/sq ft
- r radius, ft
- T temperature, °R
- w weight-flow rate, lb/sec
- η efficiency of compression (equation (1))
- ρ mass density, slugs/cu ft
- ϕ temperature-difference ratio, $\frac{T_{g,e} - T_B}{T_{g,e} - T_{a,e,h}}$
- ω angular velocity, radians/sec

Subscripts:

- a blade-cooling air
- B cooled blade
- e effective
- eq equivalent
- g combustion gas
- H hub of rotor
- h root of blade
- m mixture of combustion gas and cooling air in tail pipe of engine
- O NACA standard sea-level air
- r rotating
- s stationary
- T tip of air-cooled blade

APPARATUS AND INSTRUMENTATION

Corrugated-Fin Blade with Insert

The corrugated-fin blade with insert was a twisted blade with its internal cooling surface increased by fins made from a thin sheet of corrugated steel. An insert was incorporated to limit the cooling-air flow to the region adjacent to the blade shell in an effort to make more efficient use of the cooling air. Figure 1(a) shows the blade and indicates its twist, figure 1(b) illustrates the construction of the blade, and figure 1(c) shows the cross-section at the tip. The blade had a span of $3\frac{15}{16}$ inches and a chord of approximately $1\frac{3}{4}$ inches. The blade profile at the root was that of the standard blade for the engine, with the leading and trailing edges rounded off; the tip profile was made thicker to accommodate the cooling passage. The degree of twist was essentially the same as on the standard blade.

2578

The shell was formed from two uniformly tapered sheets of SAE 4130 steel and had a 0.053-inch thickness at the root and a 0.013-inch thickness at the tip. The pressure and suction surfaces were formed separately, after which corrugated sheets of 0.010-inch SAE 1020 steel were fitted and tack-welded to the two halves of the blade shell. The corrugations were on 3/16-inch centers and gave the sheets an over-all thickness of 0.065 inch. The two sections were then assembled about the insert of 0.010-inch SAE 1020 steel and welded together along the leading and trailing edges. The corrugations were then copper-brazed to the insert and shell, and at the same time the shell was Nicrobrazed to the SAE 4130 steel base. A dry-hydrogen-atmosphere furnace was used for this operation. The brazing served as a normalizing operation; upon removal from the furnace the blade was air-cooled, reheated, drawn at 1225° F for four hours and then air-cooled. A fillet of Eutectic 16 was then added at the root to reduce stress concentrations in this region of the blade shell during operation (see fig. 1(b)).

In order to obtain blade wall temperatures, eight chromel-alumel thermocouples were buried in the walls at a section approximately one-third span ($2\frac{9}{16}$ in. from the tip) at the peripheral locations indicated on figure 2. The details of thermocouple construction and installation are given in reference 2.

Engine

The modifications to the production turbojet engine used in this investigation were the same as described in reference 2, except that the cooled-blade configuration was different and standard production turbine blades were used immediately adjacent to the cooled blade. A single cooled blade was employed; the unused cooling passage on the disk, which could accommodate two air-cooled blades, was blocked at the hub of the disk.

The engine and test-cell instrumentation was as described in reference 2, except that thermocouple locations on the air-cooled blade were changed. The two thermocoupled solid blades used to measure effective gas temperature were placed 90° ahead of and behind the air-cooled blade rather than adjacent to it, and the blade cooling-air temperature was measured at the root of the cooled blade. No cooling-air temperature measurement was made in the inlet tube at the hub of the rotor.

Pressure-Drop Apparatus

During the investigation on the engine, no measurements of cooling-air pressures were made. Consequently, a static setup was made to obtain data on the pressure losses through the blade. This apparatus is

shown in figure 3. The modified turbine rotor and tail cone were those used in the investigation of blade-temperature distribution in the engine, so that the air-induction system would be identical for both the rotating and static phases of the investigation. Laboratory service air at 125 pounds per square inch flowed through an automatic pressure-regulating valve, a calibrated rotameter, a hand-operated control valve, the tail cone, the cooling passage along the face of the rotor, and then through the hollow turbine blade. The air was discharged into the room.

The instrumentation within the cooling-air passage is indicated in figure 3. A total-head tube, a wall static tap, and an iron-constantan thermocouple were installed in the inlet duct along the center line of the tail cone 9 inches upstream of the hub of the turbine disk. A total-head tube was also installed in the same duct 1/2 inch ahead of the disk hub. A total-head tube was employed in the cooling-air passage at the rim of the disk during tests with the blade removed to determine pressure losses in the system up to the blade root. The pressure at the blade tip was assumed to be atmospheric.

Pressures were measured on mercury manometers when above 2 inches of mercury and on water manometers when below that value. Ambient pressure was obtained from a recording barometer. Temperatures were read directly from a self-balancing potentiometer.

PROCEDURE

Experimental Procedure

Engine tests. - Air-cooled-blade temperatures were observed at constant engine speeds of 4000, 6000, 8000, 10,000, and 11,500 rpm. The blade cooling air was varied by increments from roughly 0.015 to 0.07 pound per second at each speed. All runs were made with a wide-open tail-cone nozzle. During each run, blade temperatures and cooling-air and engine-mass-flow data were obtained. Because the thermocouple pickup could handle only six thermocouples at a time, two sets of runs were required at each speed to secure data from all the cooled-blade thermocouples.

Pressure-drop investigation. - In this investigation the pressure drop through a given cooled-blade configuration was determined from measurements of the difference between the pressure drop from the central supply tube to the blade tip with the blade in the disk and the pressure drop from the central supply tube to the rim of the disk with the blade removed. This procedure avoided an otherwise difficult instrumentation problem in the passage at the disk rim. In order to obtain the relation between flow rate and pressure drop through the

system, the pressure in the central supply tube was varied by increments to yield air-flow rates ranging from 0.015 to 0.09 pound per second. Data were taken at each increment to permit evaluation of flow rate, inlet density, and pressure drop through the system. During all runs the apparatus and air were at approximately room temperature.

Measurements of total pressure within the coolant supply passage through the rim of the disk were made with the turbine blade removed. With an arbitrary air-flow rate, the total-head tube was shifted about in the passage until a maximum total-pressure reading was obtained. The tube was then clamped in place and the flow rate was varied by steps over a range from 0.015 to 0.065 pound per second.

Calculation Procedure

Blade-temperature correlation. - Blade temperatures were correlated by the procedure outlined in reference 2. The nondimensional temperature-difference ratio

$$\phi = \frac{T_{g,e} - T_B}{T_{g,e} - T_{a,e,h}}$$

which is a measure of cooling effectiveness, was plotted against the cooling-air-to-combustion-gas flow ratio w_a/w_g for each thermocouple on the blade for a given value of w_g .

This method of correlation neglects small variations in the exponents of the Reynolds numbers and in the ratios of T_g/T_B and T_a/T_B for the gas-to-blade and the blade-to-coolant heat-transfer coefficients. For most purposes these effects are negligible, so that a plot of ϕ against w_a/w_g provides a satisfactory correlation; however, care must be exercised if ϕ is used for predicting blade temperatures at gas temperatures or coolant temperatures greatly different from test conditions. In general, increase in gas temperature results in optimistic blade-temperature predictions, while increase in coolant temperature results in pessimistic blade-temperature predictions. Increases in both gas and coolant temperatures can result in either optimistic or pessimistic blade-temperature predictions, depending on the relative changes in gas or coolant temperature.

Comparison of temperature distribution of the corrugated-fin blade with that of other blades. - Inasmuch as the temperature-difference ratio ϕ is a function of engine weight flow w_g , and w_g varies with ambient

conditions, some method of correcting for these variations is required before data can be compared on a common basis; the following method was employed. The experimentally determined values of ϕ at each thermocouple location were plotted against the flow ratio w_a/w_g with w_g as a parameter. Cross plots of ϕ against w_g were made for the constant value of w_a/w_g for which a comparison was desired. From these cross plots, the w_g at which a comparison was to be made was known, and corresponding values of ϕ were obtained. Local blade temperatures were then calculated from these values of ϕ for the effective gas and cooling-air temperatures at the comparison conditions.

Comparisons of the temperature distribution of the corrugated-fin blade were made with that of two untwisted shell-supported air-cooled blades, namely a cast X-40 blade with 15 fins extending from pressure to suction surfaces (reference 1) and a formed SAE 4130 blade with 10 tubes brazed within the coolant passage (blade 12, reference 9). The corrugated-fin blade was twisted to a degree closely approximating the standard engine blades and was mounted in the turbine between two standard blades during the experimental phase of this investigation. The 15-fin untwisted blade was mounted in the turbine between two uncooled, untwisted blades of the same shape. The tube-filled untwisted blade was installed between two standard twisted blades when tested. According to results reported in references 7 and 8, the changes in flow conditions resulting from the use of twisted standard blades alongside untwisted cooled blades has little effect on cooled blade temperatures; consequently, the effects of twist on the comparisons made in this report are expected to be negligible. The 15-fin blade was selected for comparison because it is the only other finned blade that has been investigated at the NACA. The formed 10-tube blade was selected because it represents the best of the tube-filled blades which the NACA has investigated up to the present time. These comparisons were made at an engine weight-flow rate of 60.6 pounds per second which corresponds to an approximate engine speed of 10,000 rpm, a cooling-air-to-gas flow ratio of 0.029, an effective gas temperature of 1075° F, and a cooling-air temperature at the blade root of 133° F. Data at 10,000 rpm were used because there were none available for the 15-fin blade (reference 1) at higher speeds.

A comparison is also made herein of the temperature distributions of the corrugated-fin and the formed 10-tube blades with those of an air-cooled blade which employed a finned strut within the cooling-air passage to support the blade shell. In the investigation of the latter blade (reference 10), blade temperatures were measured on the mean camber line of the internal strut rather than in the blade shell. In order to compare the temperature distribution of the load-carrying member of a shell-supported blade with that of the strut-supported blade, it was expedient to average arithmetically the measured wall temperatures

at corresponding locations on the suction and pressure surfaces of the former blade and plot the results against chordwise position on the blade. Blade temperatures for both the shell-supported blades and the strut-supported blade were calculated as previously outlined for an engine weight flow of 71.4 pounds per second, which corresponds to an approximate engine speed of 11,500 rpm, an effective gas temperature of 1450° F, an effective cooling-air temperature at the blade root of 180° F, and a coolant-flow ratio of 0.03.

Comparison of stress ratio factors of the corrugated-fin blade with those of other blades. - The evaluation of the stresses in a turbine blade in operation is complicated by chordwise temperature variations and thermal and vibrational stresses. In the past the cooling effectivenesses of blades have been compared on the basis of blade temperatures alone. In reference 9, a basis of comparison was proposed which attempted to consider temperature gradients, blade material, and blade stress. The method utilized a plot of local allowable stress (based on stress-rupture data and measured local blade temperatures) against blade chord or perimeter. The ratio of the integrated average calculated allowable stress from the area under such a plot to the calculated average centrifugal stress at the same blade section is defined as a stress ratio factor. The higher the stress ratio factor for a given blade configuration, the stronger and more enduring the blade should be. Admittedly only a first approximation, the stress ratio factor should provide a better method for comparing blades of similar size and construction under comparable operating conditions than a comparison of blade temperatures only.

In the present case, where blades are of different materials, a stress ratio comparison has been made assuming all blades to be made of Timken 17-22A(S). The 100-hour stress-rupture data for this material as shown in reference 10 have been used. Average chordwise temperature distributions at rated speed and common operating conditions were calculated as previously outlined for a series of coolant-flow ratios for the corrugated-fin, the internal-strut-supported, and the formed tube-filled shell-supported blades. Operating conditions assumed were 11,500 rpm engine speed, 71.4 pounds per second gas flow, and 1450° F effective gas temperature. Two cooling-air temperatures were used, 180° F which was typical of the temperatures encountered in the investigation and 450° F which is representative of the value which might be expected in a system where the coolant is bled from the compressor discharge and used without cooling. In addition, temperature distributions were computed for the corrugated-fin and the strut-supported blades for effective gas and coolant temperatures of 2000° and 450° F, respectively, with the same local values of φ as in the preceding calculations. Then, as previously explained, the local temperatures at

corresponding positions on the pressure and suction surfaces of the shell-supported blades were averaged arithmetically and used to determine local allowable stresses from the 100-hour stress-rupture curve for Timken 17-22A(S). The calculated strut temperatures of the strut-supported blade were used directly for this purpose. The stress ratio factors were calculated as previously outlined for each blade and each condition. The average centrifugal stresses used in these calculations were computed for a section at approximately one-third span and, in each case, were based on the actual dimensions of the experimental blade.

Comparison of pressure losses of the corrugated-fin blade with those of other blades. - In order to compare the pressure losses of the corrugated-fin and the tube-filled shell-supported blades, which were measured in a stationary setup, with the pressure losses of the 15-fin shell-supported and the internal-strut-supported blades, which were based on measurements taken in the engine under operating conditions, it was necessary to place the data on a common basis. To accomplish this end, the pressure rise through the system due to rotation was calculated and eliminated from the data obtained under rotating conditions, while a density correction was made to the data obtained from the blades in the stationary setup to compensate for the lack of heat input to the air as it passed through the system. The details of these computations are given in the following paragraphs.

The method used for correlation of the cooling-air pressure losses from the disk hub to the blade tip for the rotating turbine is developed in reference 1, which gives the following expression for the equivalent nonrotating total-pressure drop corrected to a common cooling-air density at the disk hub:

$$(p'_{a,H} - p'_{m})_{0,eq} = \frac{\rho_{a,H,r}}{\rho_0} \left[p'_{a,H,r} - \left(p'_{m,r} - \frac{\eta\omega^2 r_T^2 \rho_{a,H,r}}{70.73} \right) \right] \quad (1)$$

The term $(p'_{a,H} - p'_{m})_{0,eq}$ is the equivalent nonrotating total-pressure drop, since the effects of rotation have been eliminated by the term

$$\frac{\eta\omega^2 r_T^2 \rho_{a,H,r}}{70.73}$$

In order to determine the pressure loss from the root to the tip of the rotor blade, the pressure loss from the hub of the disk (central supply tube) to the blade root, as determined from tests on a stationary rotor, was subtracted from the over-all pressure loss as given by equation (1) to obtain

$$\left(P'_{a,h} - P'_{m} \right)_{0,eq} = \left(P'_{a,H} - P'_{m} \right)_{0,eq} - \frac{\rho_{a,H,s}}{\rho_0} \left(P'_{a,H,s} - P'_{a,h,s} \right) \quad (2)$$

The values of the quantity

$$\frac{\rho_{a,H,s}}{\rho_0} \left(P'_{a,H,s} - P'_{a,h,s} \right)$$

were carefully measured in the present investigation, and lower values were obtained than have been used in previous investigations (references 3 to 7, and 10). The relative values of pressure losses for blades shown in the previous investigations are not affected by this change, because in each case a constant pressure loss from disk hub to blade root was subtracted from the over-all pressure loss for each coolant-flow rate.

In the rotating tests on the 15-fin and the strut-supported blades the cooling air was heated in flowing through the supply tubes along the face of the disk; in the stationary tests on the corrugated-fin and the tube-filled blades the disk was at approximately the same temperature as the air, and consequently there was no heat input to the air. Before root-to-tip pressure-loss data for blades tested at room temperature were compared with those from blades tested under engine operating conditions, it was necessary to account for the density changes which resulted from heat input to the air in one case and none in the other. The magnitude of the required correction was evaluated by investigating in the stationary room-temperature setup the 15-fin and other blades that had previously been investigated at rotating conditions with heat input and comparing the pressure drops with those previously obtained. It was found that the nonrotating room-temperature pressure-drop data could be correlated with the equivalent nonrotating pressure-drop data from the engine by multiplying the inlet density by a constant factor of 0.79 in the case of the room-temperature tests. This correction was therefore used on the data for the corrugated-fin and the tube-filled blades, resulting in a decrease in the density which would be the same as would be caused by an increase in cooling-air temperature due to heat input of approximately 140° F.

RESULTS AND DISCUSSION

The results of a blade-temperature-distribution investigation in a turbojet engine and a blade-pressure-loss investigation in a stationary setup are presented in this section for the corrugated-fin blade.

Temperature-distribution data are presented in figures 4 to 6; stress ratio factors are shown in figures 7 and 8; and pressure losses are given in figure 9. The data presented and the comparisons made are for the specific experimental blades used in the NACA investigations; additional research and development can undoubtedly produce improvements in the types of blades discussed herein.

Temperature-Distribution Investigation

Blade-temperature correlation. - Values of the nondimensional temperature-difference ratio ϕ have been plotted against the cooling-air-to-combustion-gas flow ratio in figure 4 for each blade thermocouple for a series of combustion-gas-flow rates. Temperature data are limited at positions 3 and 5 and lacking at position 6 as the result of thermocouple failures during operation. These figures present all the temperature data that were obtained during the investigation; cross-plots of these curves were used for all other plots and computations for the corrugated-fin blade.

In general, the data from each thermocouple location are well grouped with only small variations with combustion-gas-flow rate. In each case the values of the temperature-difference ratio ϕ first increase with increasing gas flow and then decrease. The changes in combustion-gas-flow rates are primarily due to changes in engine speed; at a given speed, changes in inlet conditions affect the gas weight-flow rate to a lesser degree. It is felt that the changes in angles of attack of the rotor blades as engine speed was varied may be responsible for the major part of the spread of the ϕ data shown in figure 4. This effect would be particularly applicable to the leading edge and the portion of the suction surface near the leading edge, where flow conditions and therefore heat-transfer rates are more readily affected by changes in angle of attack than any other portion of the blade. The spread of ϕ data is greater for the thermocouples in this region (locations 1 and 2) than for any other thermocouple except that on the suction surface at the trailing edge (location 5). The lack of correlation of ϕ data at thermocouple position 5 may be due to the variations in flow conditions and possibly to separation occurring in the rapidly diverging flow channel which resulted when the thicker cooled blade was placed between two standard uncooled blades.

The modified turbine-disk configuration was such that the cooling-air tube directed the cooling air toward the leading edge of the blade. The rapid drop of ϕ shown by thermocouples 1 and 2 at low coolant-flow ratios may be due to the low velocities of the cooling air at those points, which caused a smaller proportion of the flow to be forced toward the leading edge of the blade.

2578

Comparison of temperature distribution of the corrugated-fin blade with that of other blades. - The chordwise temperature distribution of the corrugated-fin blade is compared in figure 5 with that of a formed SAE 4130 tube-filled shell-supported blade (blade 12, reference 9) and a cast X-40 blade with 15 fins extending from suction to pressure surfaces (reference 1). As previously mentioned, the SAE 4130 shell-supported blade represents the best tube-filled blade that has been investigated by the NACA up to the present time, while the cast X-40 is the only finned blade other than the corrugated blade which has been investigated by the NACA. Blades with special provisions for cooling the leading and trailing edges have been investigated by the NACA (references 4 to 7), but the attendant stress and fabrication complications made production or operation, or both, impractical. Consequently the results of these investigations were not compared with the results obtained from the corrugated-fin blade.

The temperature distributions (fig. 5) were compared at effective gas and cooling-air temperatures of 1082° and 110° F, respectively, a coolant flow ratio of 0.026, and an engine weight-flow rate of 63.4 pounds per second which corresponds approximately to an engine speed of 10,000 rpm, the maximum speed at which the 15-fin blade was operated. Under these conditions the integrated average temperature of the corrugated-fin blade was 619° F as compared with 633° F for the cast 15-fin blade. The leading- and trailing-edge temperatures of the corrugated-fin blade were approximately 110° and 230° F lower than those of the 15-fin blade. In the midchord regions the temperatures of these two blades were nearly the same on the pressure surface, but the 15-fin blade was as much as 100° F lower on the suction surface. The average temperature of the corrugated-fin blade was 75° F cooler than that of the tube-filled blade (619° against 694° F), and its leading edge was approximately 100° F cooler; however, the corrugated-fin blade trailing edge was approximately 75° F hotter than that of the tube-filled blade.

In comparing these blades, three pertinent factors must be kept in mind. The methods of construction employed probably resulted in better thermal bonds between the fins and the shell of the 15-fin blade than were obtained in the corrugated-fin and the tube-filled blades. When the 15-fin blade was made, the fins were fitted into individual slots before brazing, while in the fabrication of the other blades the tubes and corrugations were inserted into completed shells from the blade tips with no positive provisions for ensuring adequate thermal contact with the shell at all points. The second factor, which also stems from blade construction methods, is that the corrugated-fin and tube-filled blades were formed from sheet metal, and it was possible to extend the cooling passages farther into the leading and trailing edges than was possible with the casting process used in making the shell of the 15-fin blade. The third factor lies in the differences in the internal cooling-passage configurations. The corrugated-fin blade employed an insert which forced

the coolant to flow through a narrow peripheral band adjacent to the shell, whereas the 15-fin blade coolant passage was made up of a group of nearly rectangular passages extending from the pressure to the suction surface. The tube-filled blade coolant passage was more restricted than that of the 15-fin blade but not nearly to the extent of that of the corrugated-fin blade. These variations in coolant-passage configurations will affect not only the coolant velocity due to area differences but also the distribution of cooling air within the passage. For a given total coolant-flow rate, the amount of air flowing through the leading- and trailing-edge regions should be greater for the corrugated-fin blade than for the 15-fin blade, while that for the tube-filled blade should lie between the two.

These considerations explain, for the most part, the relative temperature distributions shown in figure 5. The higher thermal bond and greater coolant flow in the midchord region explains the lower temperatures in that part of the 15-fin blade; the reduced flow at the leading and trailing edges accounts for the higher temperatures there. The greater cooling effectiveness of the corrugated-fin blade as compared with the tube-filled blade probably results from higher coolant velocities and the concentration of the total coolant flow in the region immediately adjacent to the shell and the bases of the corrugations. It was thought that for a given coolant-flow rate the construction of the corrugated-fin blade would yield wall temperatures lower at every corresponding point than those obtained with the formed tube-filled blade. Actually, this was the case for all locations except the trailing edge; here it is believed that in the process of welding the two halves of the corrugated-fin blade together, the coolant passage was restricted and an uncooled length of trailing edge (measured in a chordwise direction) was obtained which was longer than that of the tube-filled blade. The effects of the longer uncooled lengths have been noted previously; reference 9 discusses the point.

The reduction of leading- and trailing-edge temperatures is significant in that thermal stresses are reduced. A blade with a relatively uniform wall-temperature distribution may be operated at a higher stress level than one with greater peripheral wall-temperature variations. In addition, when uncooled blades of low-alloy steels (so-called non-strategic blades) are used, the reduction of leading- and trailing-edge temperatures is of great significance in decreasing the rates of oxidation.

The chordwise temperature distributions at rated engine conditions for the load-carrying members of the internal-strut-supported blade (reference 10), the formed tube-filled shell-supported blade (reference 9), and the corrugated-fin blade are shown in figure 6 for a coolant-to-gas flow ratio of 0.03. In the NACA air-cooled-blade investigations, only on these three blades have temperature distributions

2578

been measured at rated speed (reference 7 reported temperatures at two locations on a fourth blade at 11,500 rpm). The shell-supported blade temperatures were averaged as explained in the section under PROCEDURE. It is at once evident from figure 6 that the cooling effectiveness of the internal-strut-supported blade is much greater than that of the two shell-supported blades. At the coolant-to-gas flow ratio of 0.03 the integrated average temperature of the internal-strut-supported blade was 615° F as compared with 838° F for the corrugated-fin blade and 930° F for the formed tube-filled blade. As at 10,000 rpm, the cooling effectiveness of the corrugated-fin blade was superior to that of the formed tube-filled blade; in each case local blade temperatures of the latter were lower only near the trailing edge.

Temperature differences of the magnitude shown between the strut-supported blade and the shell-supported types are very significant when the strength of current turbine-blade materials in the temperature range above 900° F is considered. If either the gas or coolant temperature were increased to the point at which the strut of the strut-supported blade reached the neighborhood of 1000° F, at these same engine conditions the corrugated-fin and the tube-filled blade shells would be in a temperature range in which safe operation would be impossible.

From a comparison on the basis of cooling effectiveness alone, the strut-supported blade is superior to the shell-supported types at all conditions investigated. However, since the strut-supported blade is more highly stressed because of the necessity for carrying the weight of the blade shell on the internal-strut-support member, a comparison on the basis of load-carrying ability will reduce its margin of superiority. Such a comparison is made in the following section.

Comparison of stress ratio factors of the corrugated-fin blade with those of the tube-filled shell-supported blade. - As previously mentioned, the stress ratio factors proposed in reference 9 offer a better basis for comparison of air-cooled blades for an engine application than do the blade temperature distributions. For a given blade configuration, the higher the stress ratio factor, the better the blade; for different configurations, however, vibratory, gas-bending, and thermal stresses may require consideration.

In the present investigation, comparisons have been made on the basis of 100-hour stress-rupture properties of Timken 17-22A(S) which is a low-alloy steel that shows great promise as a nonstrategic turbine-blade material. The 100-hour stress-rupture curve for Timken 17-22A(S) is given in reference 10. Stress ratio comparisons for the corrugated-fin, the tube-filled, and the strut-supported blades are shown in figure 7. (The strut-supported blade will be discussed in the next section.) The comparisons in figure 7(a) are for the same engine operating

conditions as for the temperature comparison of figure 6, in which the cooling-air temperature at the blade root was 180° F, a value representative of those encountered on the test stand. In addition, comparisons have been made in figure 7(b) on the basis of a cooling-air temperature of 450° F at the blade root, which is representative of cooling air obtained from the compressor discharge. The temperatures used for calculating the stress ratio factors for a cooling-air temperature of 450° F were computed from the experimentally determined values of the temperature-difference ratio ϕ , which were obtained with cooling air at temperatures from 50° to 200° F. The effect of assuming these local values of ϕ to be constant in calculations of blade temperatures corresponding to the increased cooling-air temperature was estimated by consideration of the theoretical heat-transfer equations involved, which indicated that the use of the constant experimental values of ϕ should yield metal temperatures about 25° F too high. It was concluded that stress ratio factors determined in this manner would therefore be conservative.

The corrugated-fin blade has higher stress ratio factors than the tube-filled shell-supported blade over the entire range of flow ratios investigated. Because the two shell-supported blades were equally stressed, their stress ratio curves in figure 7(a) may be compared directly to show the effect of the differences in cooling effectiveness which are indicated by figure 6. The stress ratio curve of the tube-filled blade is lower than and tending to become parallel to that for the corrugated-fin blade above a flow ratio of 0.04, but below that value it falls off rapidly. This fall occurs because of the shape of the Timken 17-22A(S) stress-rupture curve in which strength drops off at a rate which increases steadily with increasing temperature within the temperature range of this investigation.

At present, a minimum safe stress ratio factor has not been determined. Reference 9 reported over 25 hours of satisfactory operation at rated engine conditions on a blade with a stress ratio factor of 2.16. It is believed that a value between 1.5 and 2 will prove to be adequate. On this basis the stress ratio factors of figure 7 indicate that the corrugated-fin blade could probably operate safely over the range of conditions covered by the corrugated-fin curves. The curves of the formed tube-filled blade show that with a coolant temperature of 450° F and a coolant-flow ratio from 0.020 to 0.025, the blade is entering the critical operating region. For an estimated safe operating stress ratio factor of 2, extrapolation of figure 7(b) indicates that the corrugated-fin blade will require a coolant-flow ratio of 0.0085, while the tube-filled blade would require a coolant-flow ratio of 0.0245, an increase of nearly 300 percent.

From the foregoing it is evident that on the basis of both cooling effectiveness and stress ratio factor the corrugated-fin blade shows a clear-cut superiority over the tube-filled blade which would make it more desirable for use in a turbine engine with air-cooled blades of approximately the same profile as the blades discussed herein.

2578 Comparison of stress ratio factors of the corrugated-fin blade with those of the internal-strut-supported blade. - The corrugated-fin blade is compared on the basis of stress ratio factors with the strut-supported blade in figure 7 for the conditions outlined in the preceding section. At flow ratios above 0.01 the corrugated-fin blade has higher stress ratio factors than the strut-supported blade. Extrapolation of the data from a coolant temperature of 180° to 450° F, a value which might be obtained by bleeding cooling air from the compressor, indicates that the corrugated-fin blade has higher stress ratio factors at flow ratios above 0.024. If it is assumed that an acceptable operating stress ratio factor lies in the range from 1.5 to 2.0, both the corrugated-fin and the strut-supported blades can operate safely at coolant flow ratios less than 0.01.

The strut-supported blade, because of its much lower strut temperatures, was operating along a relatively flat portion of the stress-rupture curve; consequently there was little change in allowable stress with flow ratio in the temperature range encountered, and the stress ratio factors remained almost constant over a wide range of coolant flow ratios. The fact that the strut-supported blade had lower stress ratio factors even though it was cooler resulted from the higher stresses which are inherent in this type of design.

Results obtained by extrapolating the data to an effective gas temperature of 2000° F, a cooling-air temperature of 450° F, and a gas flow of 71.4 pounds per second at 11,500 rpm are shown in figure 8. The figure shows that as heat-transfer conditions become increasingly critical for the cooled blades, the strut-supported blade performs increasingly better in comparison with the corrugated-fin blade. Figure 8 shows that at the conditions stated previously the strut blade can operate in the stress ratio range of 1.5 to 2.0 with coolant-flow ratios of 0.01 to 0.02, while the corrugated-fin blade requires flow ratios of 0.053 to 0.065. This better relative showing of the strut blade as gas temperature increases results from two factors. First, the internal strut which carries the load of the strut blade is affected less by a change in gas temperature than the shell of the shell-supported corrugated-fin blade, and second, the allowable stress of the strut blade is affected less by a given change in metal temperature than the shell of the corrugated-fin blade because of the lower strut temperature and its position on the more nearly flat portion of the stress-rupture curve.

~~CONFIDENTIAL~~

Approximate calculations indicate that the use of constant experimental ϕ values for a given constant flow ratio in extrapolating to higher gas and coolant temperatures for the conditions in figure 8 resulted in conservative stress ratio factors as was the case for figure 7(b).

From figures 5 and 6 it is evident that the corrugated-fin blade represents an improvement in over-all cooling effectiveness over the tube-filled blade and thus over any of the shell-supported types previously investigated. Since the centrifugal stresses in each of the shell-supported types of blade were comparable, the stress ratio factors and the load-carrying ability of the corrugated-fin blade as indicated in figure 7 may be expected to be superior to those of any of the shell-supported types tested. At current gas-temperature levels the stress ratio factors indicate that the corrugated-fin blade made from available low-alloy steel is capable of safe operation at coolant-flow ratios below 0.01. At these conditions the use of the heavier, more highly stressed internal-strut-supported blades is not warranted, except possibly where turbine and cooling system designs are sufficiently critical to justify the added complications to obtain a lower cooling-air flow rate.

As gas temperatures or cooling-air temperatures, or both, increase, the greater cooling effectiveness of the strut-supported blade begins to outweigh the disadvantages resulting from its heavier construction; and successful operation is possible with reasonable coolant flows at conditions considerably beyond the limits of the corrugated-fin or other types of shell-supported blade.

The stress comparisons made in this report are based on the actual dimensions of the experimental blades investigated, each of which represents the first of its type. Design refinements can undoubtedly increase cooling effectiveness and reduce mechanical stresses. Therefore, comparisons should be made on a qualitative rather than a quantitative basis at this time.

Pressure-Loss Investigation

The pressure-loss data for the corrugated-fin blade, which were obtained in the stationary setup and corrected for heat input as explained in the Calculation Procedure, are compared in figure 9 with pressure losses through the 15-fin, the formed tube-filled, and the strut-supported blades. Data from the 15-fin and strut-supported blades were obtained during rotating tests and corrected to eliminate the effects of rotation by methods previously outlined. The corrugated-fin blade had a pressure drop twice that of the 15-fin blade at a flow rate

2578

2578

of 0.022 pound per second and 2.75 times as great at a flow rate of 0.06 pound per second, while its pressure drops were 24 percent greater than those of the tube-filled blade at both of these cooling-air flow rates. The corrugated-fin pressure drop was lower than that of the strut-supported blade by 35 percent at a flow rate of 0.016 and higher by 35 percent at 0.06 pound per second. At a cooling-air flow rate of 0.02 pound per second, which corresponds to a coolant-flow ratio of about 0.015 at rated engine conditions, the pressure drops through the corrugated-fin, the 15-fin, the tube-filled, and the strut-supported blades were 3.7, 1.75, 3.0, and 4.55 inches of mercury, respectively. The results of an investigation on a modified turbine in the same model turbojet engine in which all turbine blades were cooled (reference 11) indicate that in this engine the compressor-discharge pressures are considerably greater than necessary to supply blade-cooling air in the quantities required over the entire range of operating conditions. Thus, for most applications the pressure losses for all four blades would probably be satisfactory; therefore, the differences in pressure drops through the cooled blades would have little influence on the choice of blade types.

SUMMARY OF RESULTS

The following results were obtained in an experimental investigation of air-cooled turbine blades:

1. The corrugated-fin blade had a lower integrated average temperature at one-third span and, with one exception, lower leading- and trailing-edge temperatures than any of the previously investigated types of shell-supported air-cooled blades which appear practical from the standpoints of stress and fabrication. At sea-level conditions typical of an engine speed of 10,000 rpm and a cooling-air-to-combustion-gas flow ratio of 0.026, the integrated average blade temperature of the corrugated-fin blade at a section at approximately one-third span was 619° F. Corresponding values for the cast 15-fin and the formed tube-filled blades were 633° and 694° F, respectively. At conditions corresponding to 11,500 rpm with a flow ratio of 0.03, the average corrugated-fin blade temperature was 838° F as compared to 930° F for the tube-filled blade.

2. At current gas-temperature levels, calculations indicate that the corrugated-fin blade, if made of Timken 17-22A(S) nonstrategic steel, can operate safely at cooling-air-to-combustion-gas flow ratios of 0.01 or less with cooling-air inlet temperatures up to 450° F.

3. The cooling effectiveness of the corrugated-fin blade at rated engine conditions was inferior to that of a previously tested blade in which the air-cooled shell was supported by a finned strut within the coolant passage. The integrated average temperature of the corrugated-fin blade at 11,500 rpm, effective gas and cooling-air temperatures of 1450° and 180° F, respectively, and a cooling-air-to-combustion-gas flow ratio of 0.03 was 838° F as compared to 615° F for the strut-supported blade.

4. Comparison on the basis of stress ratio factors indicates that at 11,500 rpm with effective gas and coolant temperatures of 1450° and 180° F, respectively, the corrugated-fin blade was superior to the strut-supported blade at coolant-flow ratios greater than 0.01. Extrapolation of data to account for a coolant temperature of 450° F indicates that the strut blade is superior at flow ratios below 0.024 and that both blades are capable of safe operation below flow ratios of 0.01.

5. At 11,500 rpm with an effective gas temperature of 2000° F and a coolant temperature of 450° F, the strut-supported blade was markedly superior to the corrugated-fin blade at all flow ratios. The strut-supported blade appeared capable of safe operation with flow ratios as low as 0.02, while the corrugated blade would require a coolant flow ratio of about 0.06.

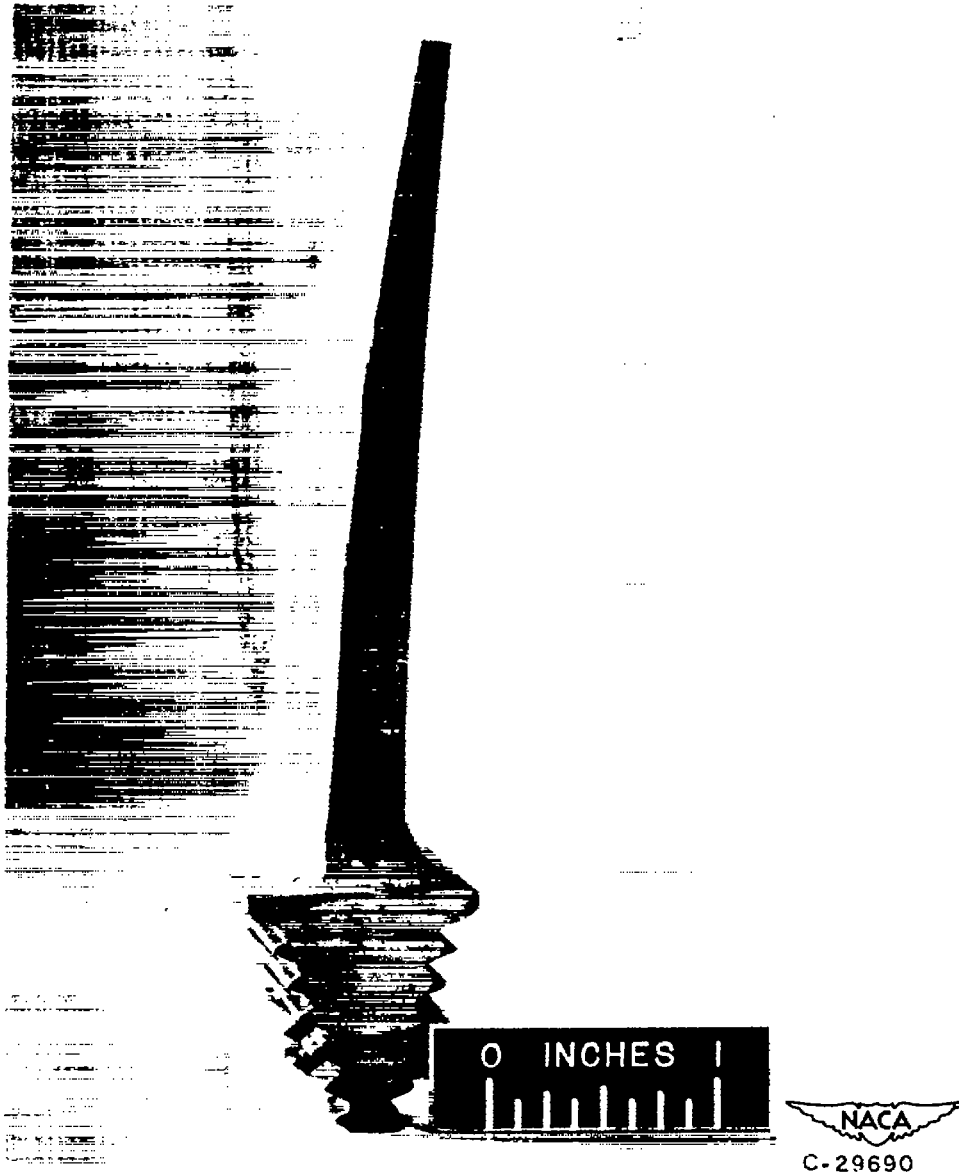
6. Pressure losses through the corrugated-fin blade were from 200 to 300 percent greater than those through the 15-fin blade, 24 percent greater than those through the tube-filled blade, and from 35 percent lower to 35 percent higher than those through the strut-supported blade over the range of air flows investigated. At a cooling-air flow rate of 0.02 pound per second the pressure drops through the corrugated-fin, the 15-fin, the tube-filled, and the strut-supported blades were 3.7, 1.75, 3.0, and 4.55 inches of mercury, respectively.

Lewis Flight Propulsion Laboratory
National Advisory Committee for Aeronautics
Cleveland, Ohio

REFERENCES

1. Hickel, Robert O., and Ellerbrock, Herman H., Jr.: Experimental Investigation of Air-Cooled Turbine Blades in Turbojet Engine. II - Rotor Blades with 15 Fins in Cooling-Air Passages. NACA RM E50114, 1950.

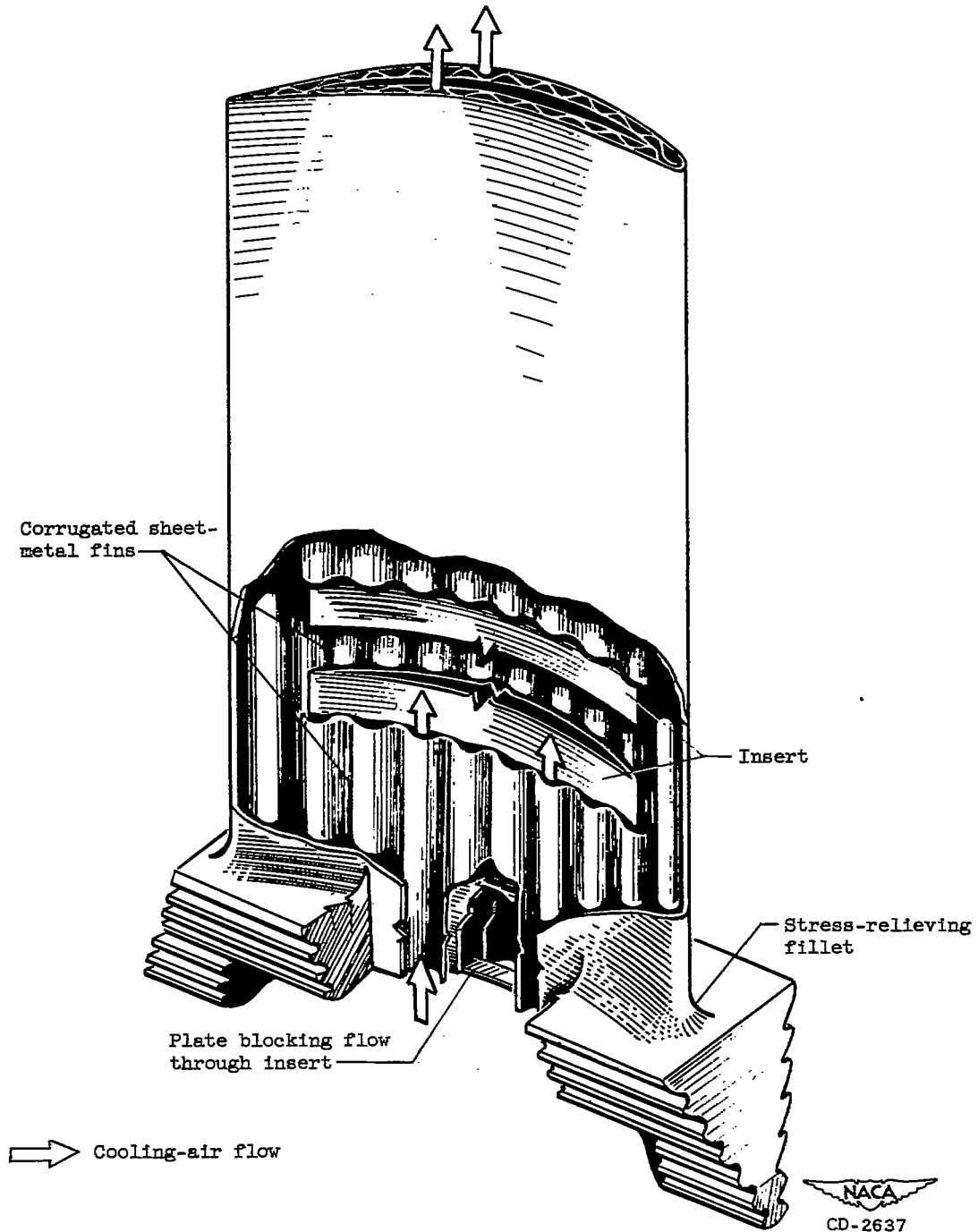
2. Ellerbrock, Herman H., Jr., and Stepka, Francis S.: Experimental Investigation of Air-Cooled Turbine Blades in Turbojet Engine. I - Rotor Blades with 10 Tubes in Cooling-Air Passages. NACA RM E50I04, 1950.
3. Hickel, Robert O., and Smith, Gordon T.: Experimental Investigation of Air-Cooled Turbine Blades in Turbojet Engine. III - Rotor Blades with 34 Steel Tubes in Cooling-Air Passages. NACA RM E50J06, 1950.
4. Ellerbrock, Herman H., Jr., Zalabak, Charles F., and Smith, Gordon T.: Experimental Investigation of Air-Cooled Turbine Blades in Turbojet Engine. IV - Effects of Special Leading- and Trailing-Edge Modifications on Blade Temperatures. NACA RM E51A19, 1951.
5. Smith, Gordon T., and Hickel, Robert O.: Experimental Investigation of Air-Cooled Turbine Blades in Turbojet Engine. V - Rotor Blades with Split Trailing Edges. NACA RM E51A22, 1951.
6. Arne, Vernon L., and Esgar, Jack B.: Experimental Investigation of Air-Cooled Turbine Blades in Turbojet Engine. VI - Conduction and Film Cooling of Leading and Trailing Edges of Rotor Blades. NACA RM E51C29, 1951.
7. Smith, Gordon T., and Hickel, Robert O.: Experimental Investigation of Air-Cooled Turbine Blades in Turbojet Engine. VIII - Rotor Blades with Capped Leading Edges. NACA RM E51H14, 1951.
8. Stepka, Francis S., and Hickel, Robert O.: Experimental Investigation of Air-Cooled Turbine Blades in Turbojet Engine. IX - Evaluation of Durability of Noncritical Rotor Blades in Engine Operation. NACA RM E51J10, 1951.
9. Esgar, Jack B., and Clure, John L.: Experimental Investigation of Air-Cooled Turbine Blades in Turbojet Engine. X - Endurance Evaluation of Several Tube-Filled Rotor Blades. NACA RM E52B13, 1952.
10. Cochran, Reeves P., Stepka, Francis S., and Krasner, Morton H.: Experimental Investigation of Air-Cooled Turbine Blades in Turbojet Engine. XI - Internal-Strut-Supported Rotor Blade. NACA RM E52C21, 1952.
11. Nachtigall, Alfred J., Zalabak, Charles F., and Ziemer, Robert R.: Investigations of Air-Cooled Turbine Rotors for Turbojet Engines. III - Experimental Cooling-Air Impeller Performance and Turbine Rotor Temperatures in Modified J33 Split-Disk Rotor up to Speeds of 10,000 RPM. NACA RM E52C12, 1952.



(a) Blade after testing.

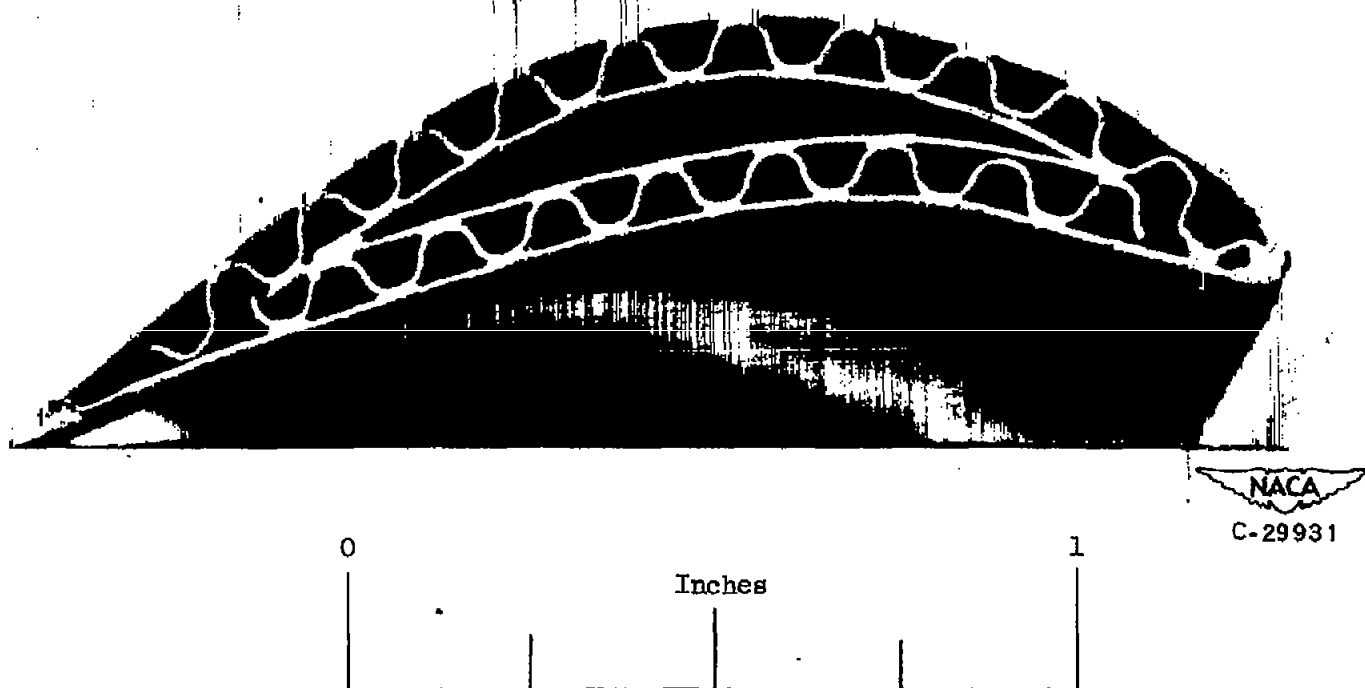
Figure 1. - Twisted corrugated-fin blade.

2578



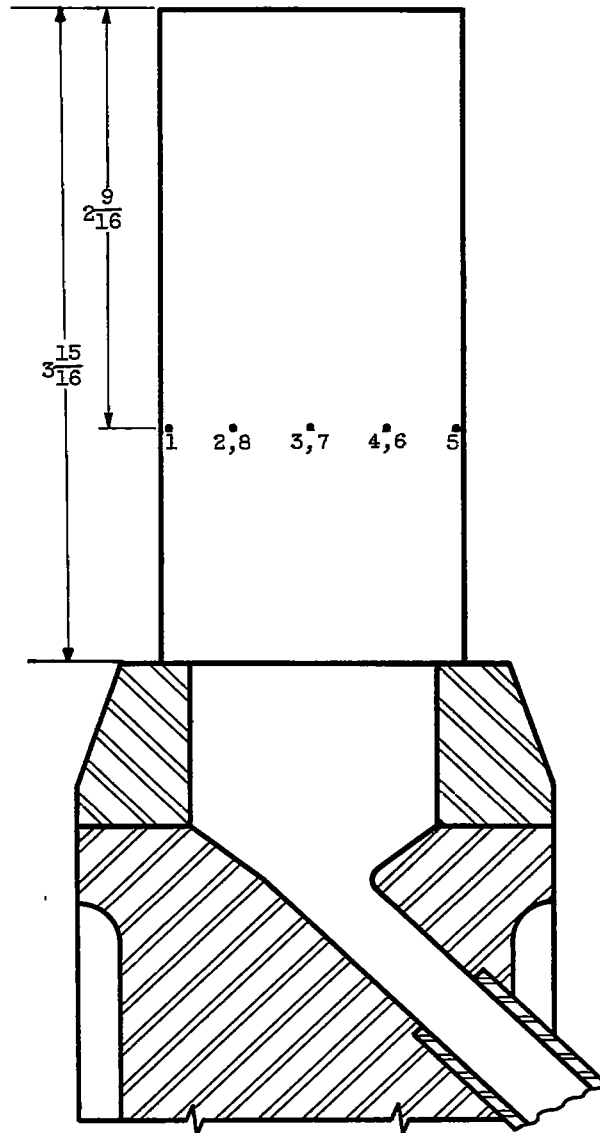
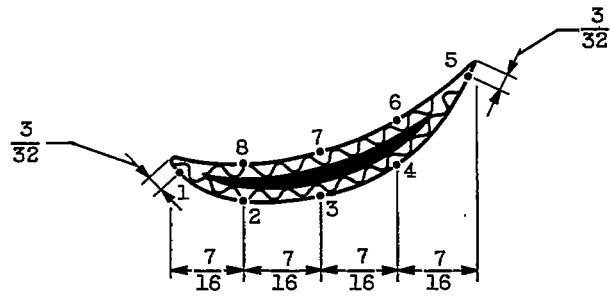
(b) Phantom view showing construction.

Figure 1. - Continued. Twisted corrugated-fin blade.



(c) Tip section.

Figure 1. - Concluded. Twisted corrugated-fin blade.



NACA
CD-2623

Figure 2. - Locations of thermocouples on the twisted corrugated-fin blade.

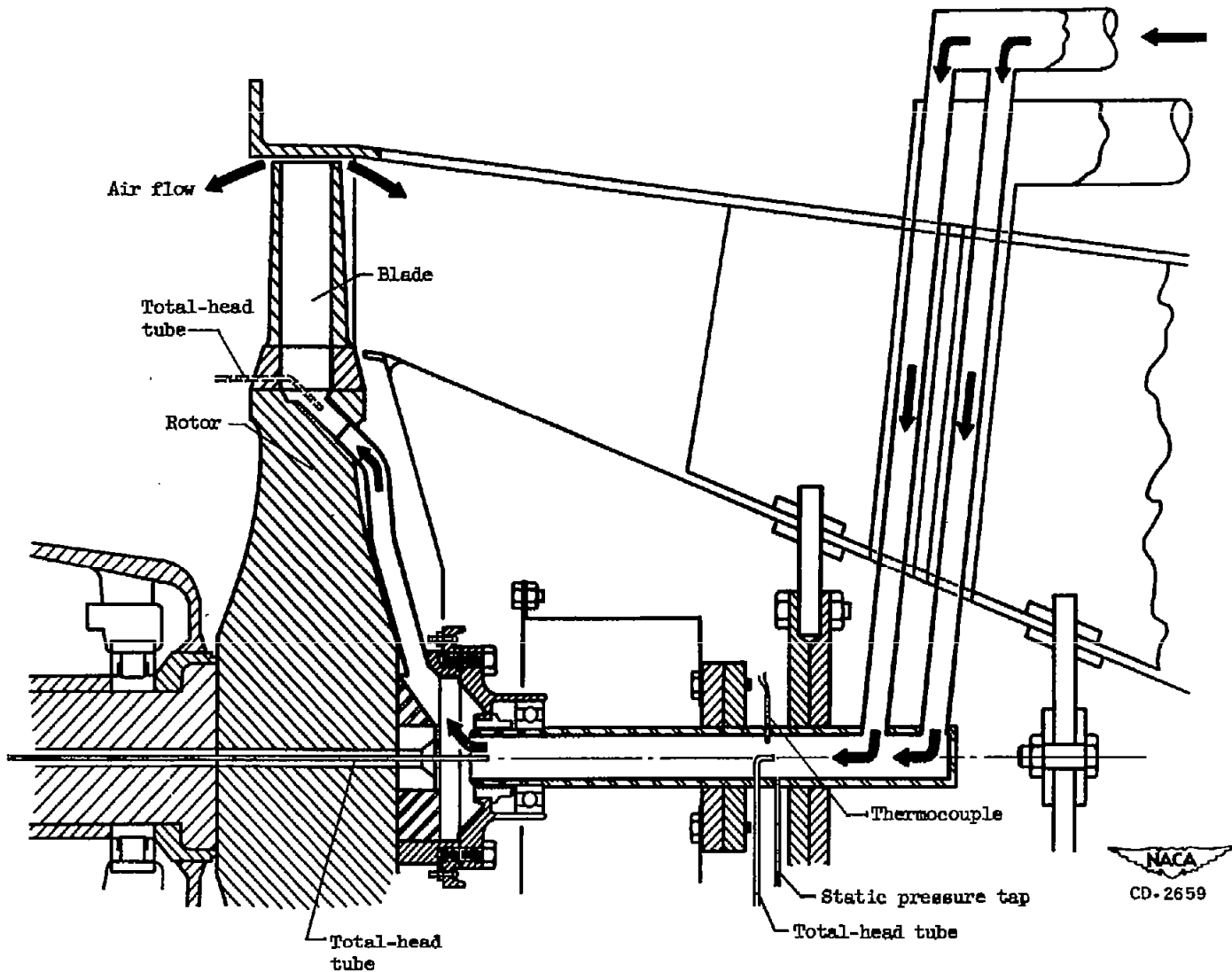
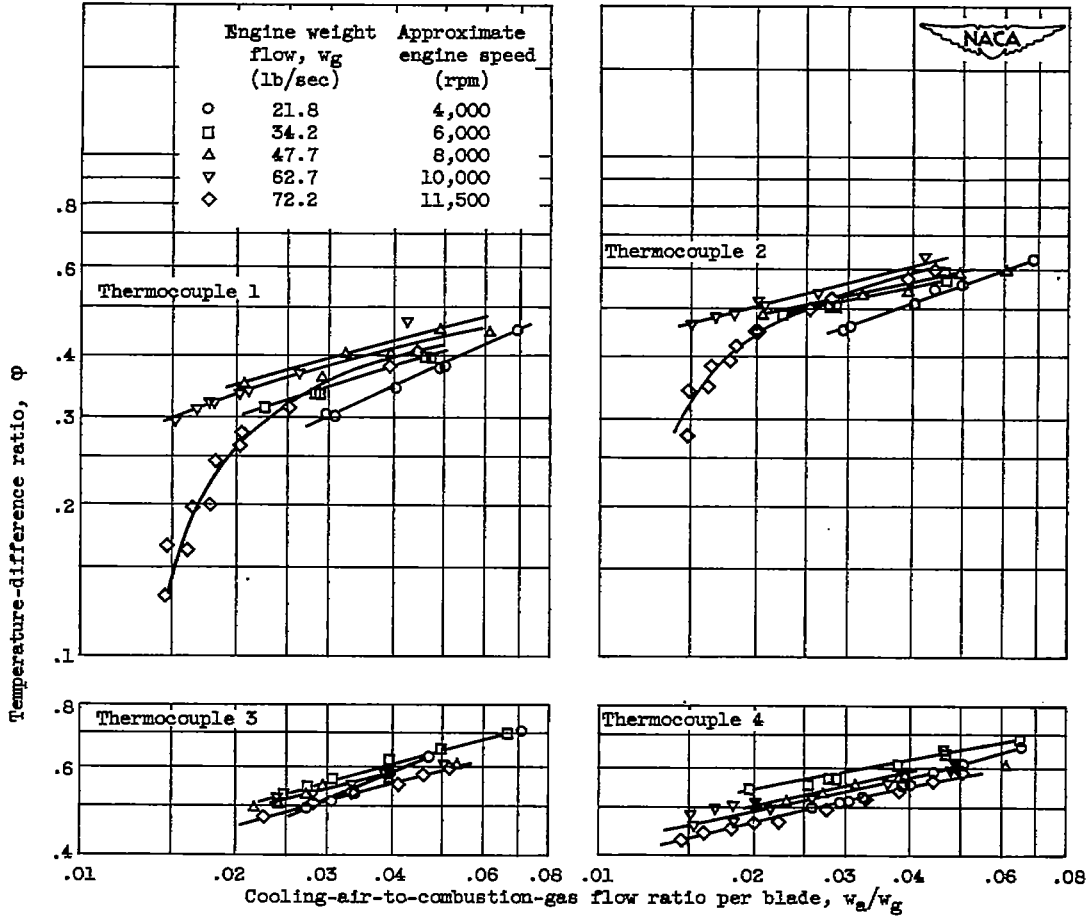


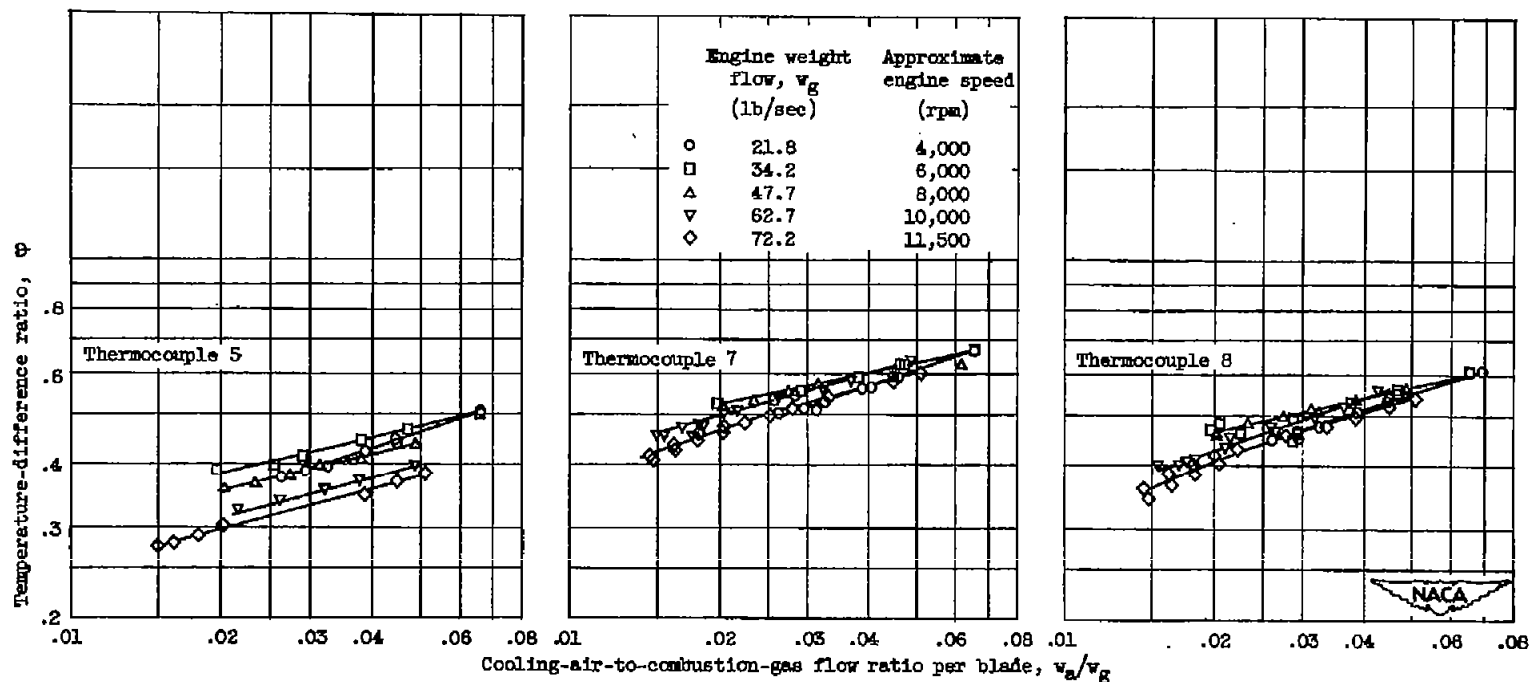
Figure 3. - Apparatus for nonrotating pressure-drop investigation.

2578



(a) Thermocouples 1, 2, 3, and 4.

Figure 4. - Variation of temperature-difference ratio with cooling-air-to-combustion-gas flow ratio per blade for range of engine weight flows w_g .



(b) Thermocouples 5, 7, and 8.

Figure 4. - Concluded. Variation of temperature-difference ratio with cooling-air-to-combustion-gas flow ratio per blade for range of engine weight flows w_g .

CONFIDENTIAL

2578

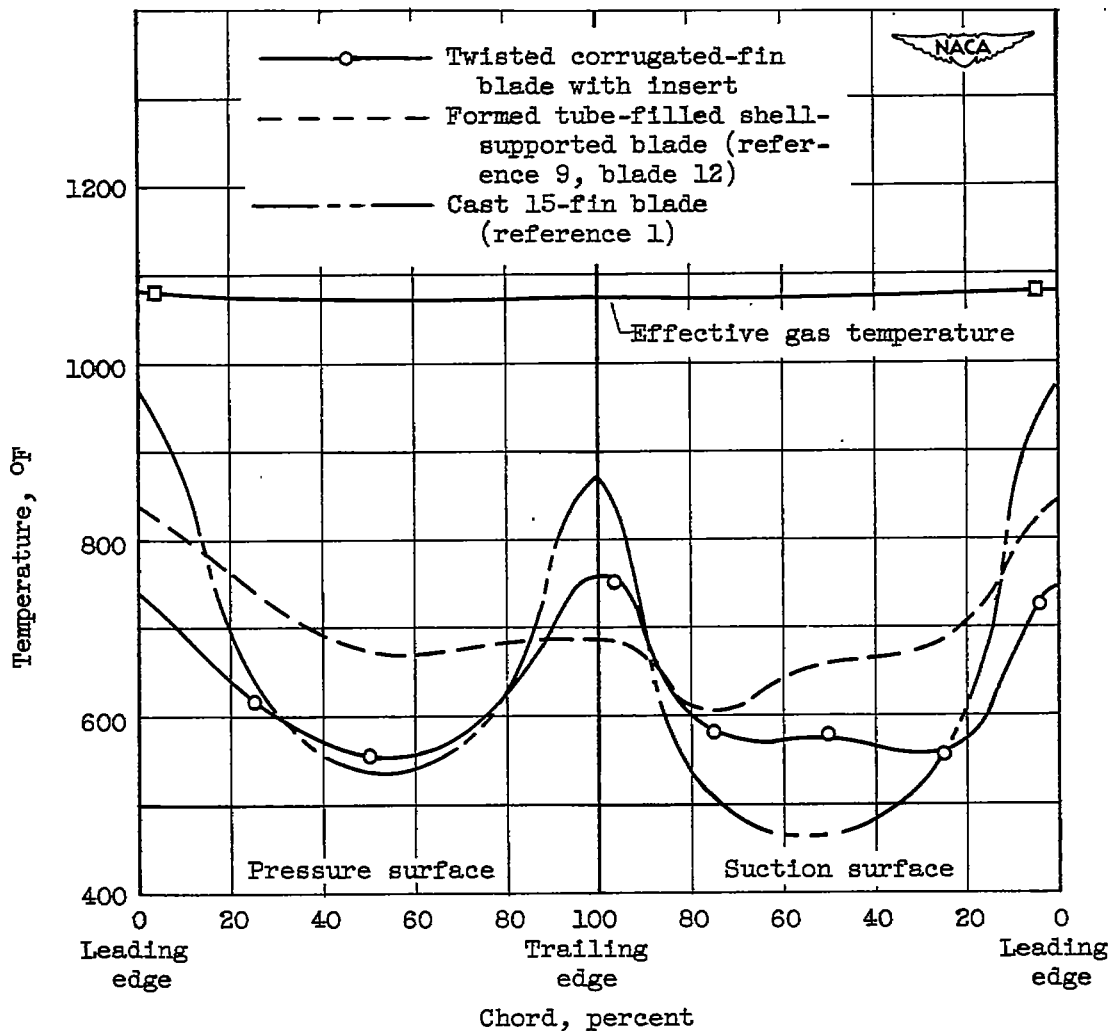


Figure 5. - Comparison of chordwise temperature distribution of corrugated-fin blade with other shell-supported types. Engine speed, approximately 10,000 rpm; combustion gas flow, 63.4 pounds per second; coolant-to-gas flow ratio, 0.026; effective gas temperature, 1082° F; cooling-air temperature at blade root, 110° F.

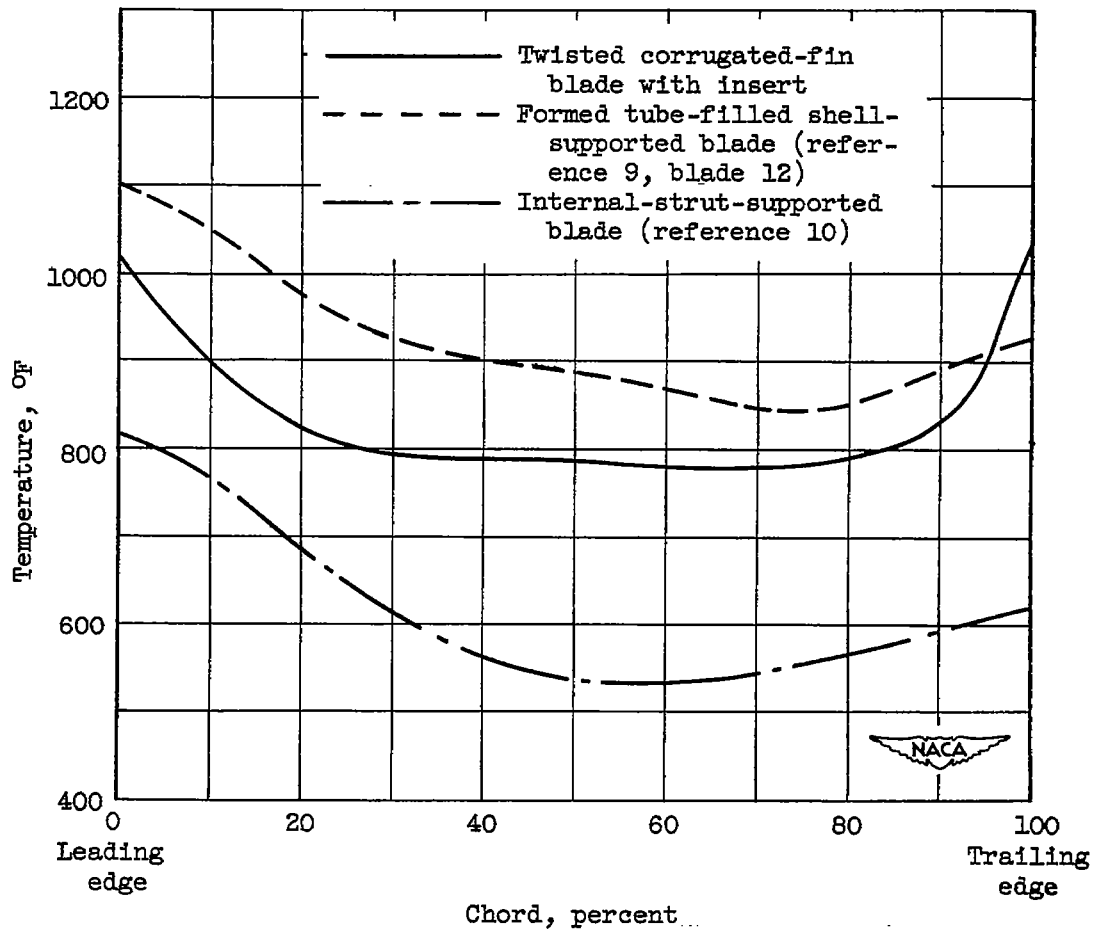
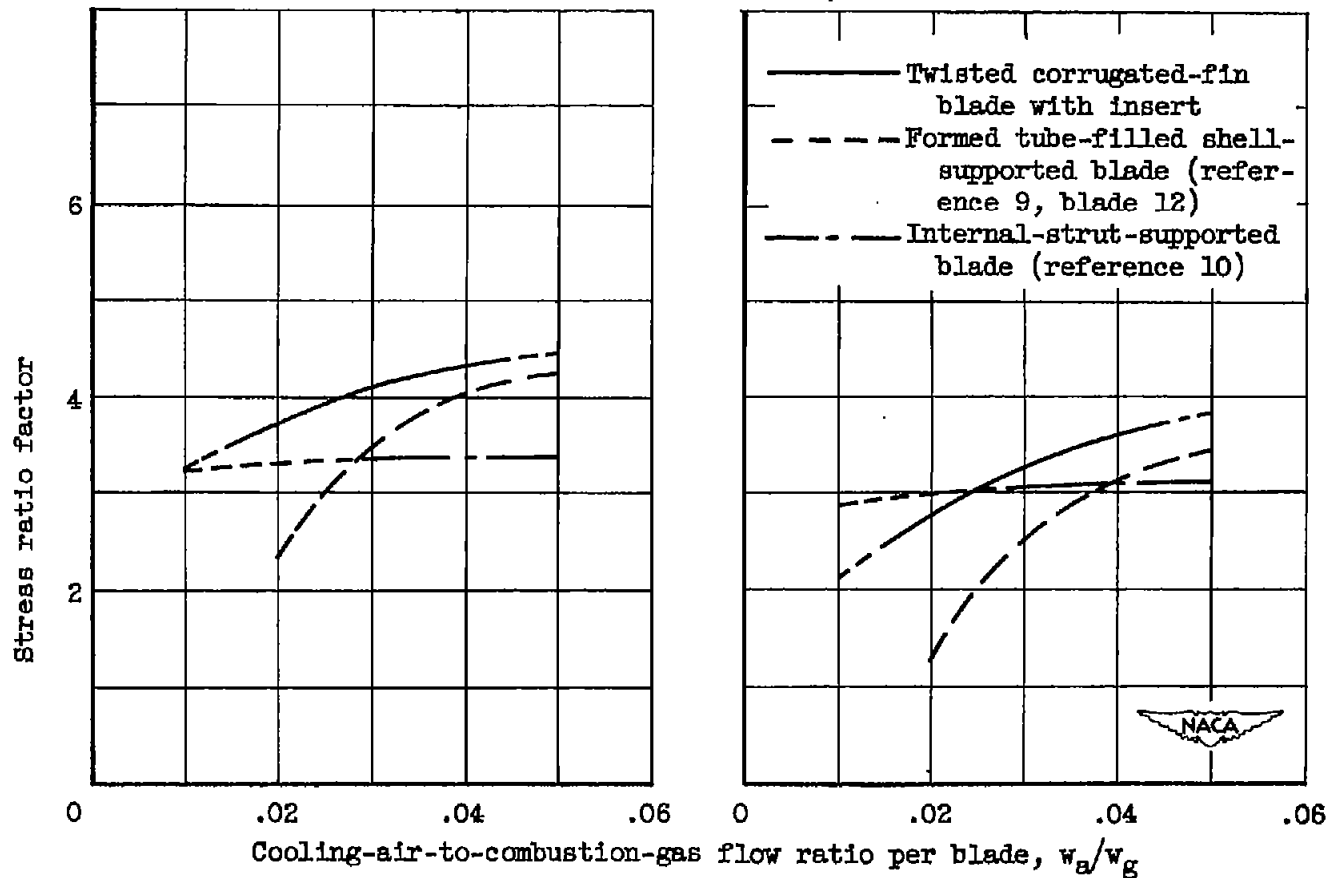


Figure 6. - Comparison of chordwise temperature distribution of corrugated-fin blade with insert with those of formed tube-filled shell-supported and internal-strut-supported blades. Engine speed, 11,500 rpm; combustion gas flow, 71.4 pounds per second; coolant-to-gas flow ratio, 0.03; effective gas temperature, 1450° F; cooling-air temperature at blade root, 180° F.



(a) Cooling-air temperature, 180° F.

(b) Cooling-air temperature, 450° F.

Figure 7. - Comparison of stress ratio factors of corrugated-fin blade with those of formed tube-filled shell-supported and internal-strut-supported blades on the basis of Timken 17-22A(S) 100-hour stress-rupture data. Engine speed, 11,500 rpm; effective gas temperature, 1450° F; gas-flow rate, 71.4 pounds per second.

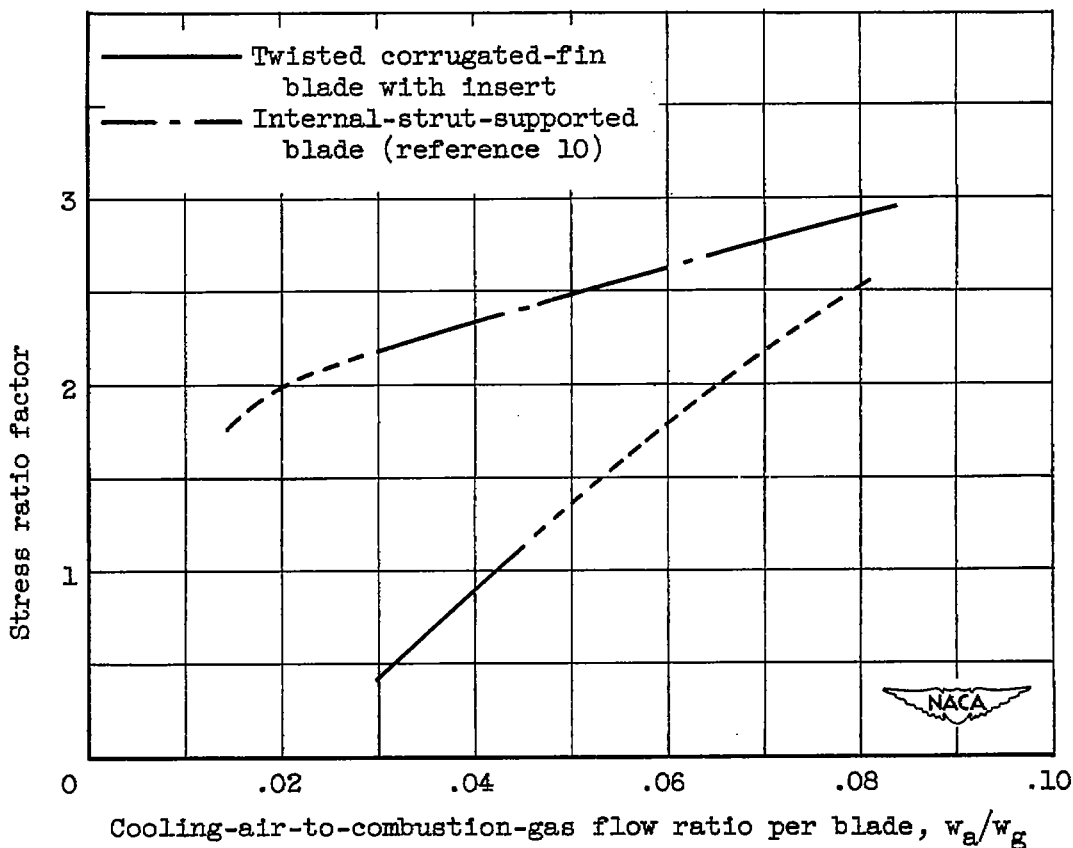


Figure 8. - Comparison of stress ratio factors of corrugated-fin blade with those of internal-strut-supported blade on the basis of Timken 17-22A(S) 100-hour stress-rupture data. Engine speed, 11,500 rpm; effective gas temperature, 2000° F; effective coolant temperature, 450° F; gas-flow rate, 71.4 pounds per second.

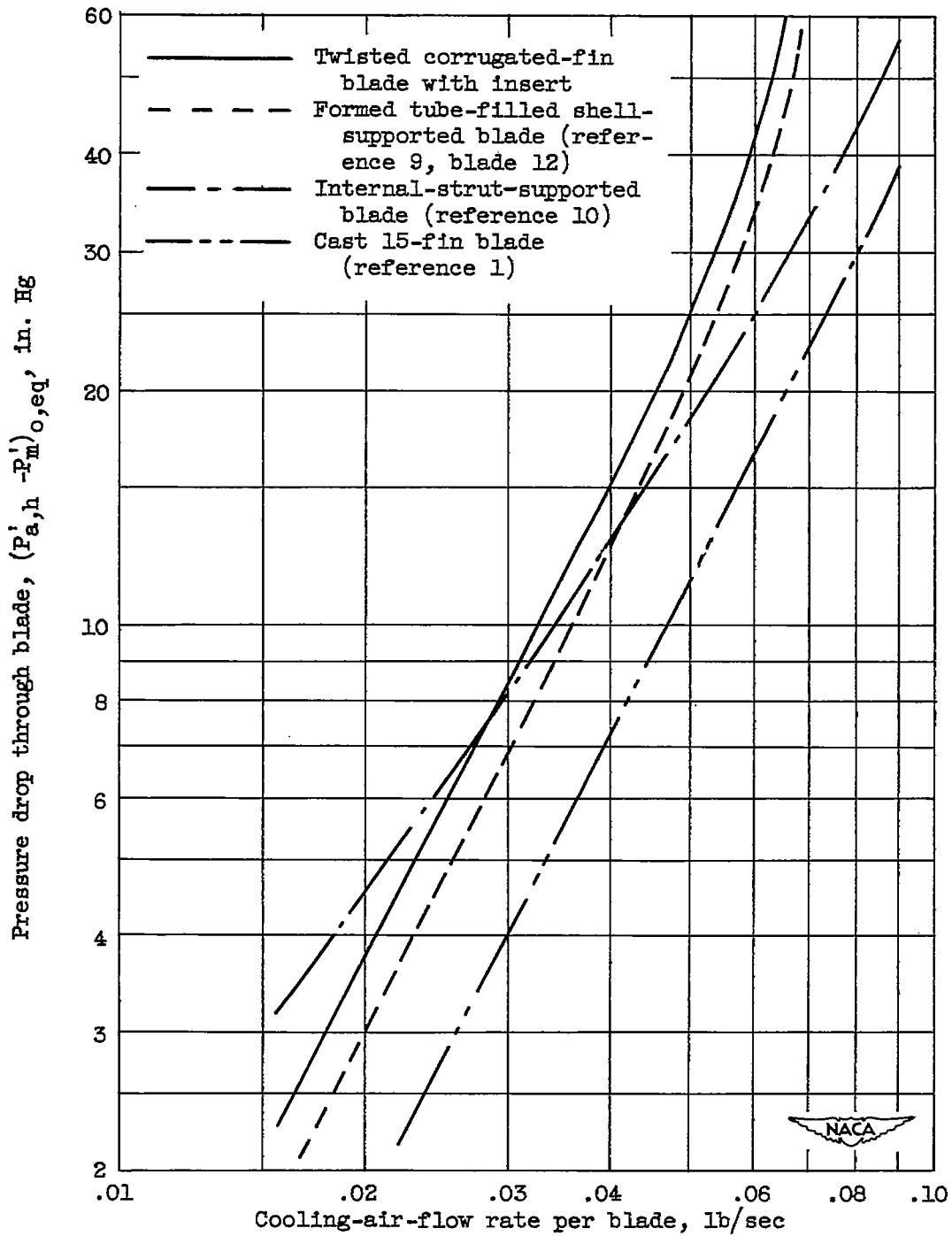


Figure 9. - Comparison of pressure losses through corrugated-fin blade with those through internal-strut-supported blade, formed tube-filled shell-supported blade, and cast 15-fin blade.